10-2018

Synthesis and Evaluation of Protein-Phenylboronic Acid Conjugates as Lectin Mimetics

Joshua Whited
Cleveland State University

Czharena Kay Rama
Cleveland State University

Xue-Long Sun
Cleveland State University, x.sun55@csuohio.edu

Publisher's Statement

ACS OMEGA

Article

Cite This: ACS Omega 2018, 3, 13467−13473

http://pubs.acs.org/journal/acsodf

Synthesis and Evaluation of Protein−Phenylboronic Acid Conjugates as Lectin Mimetics

Joshua Whited, Czharena Kay Rama, and Xue-Long Sun*

Department of Chemistry, Chemical and Biomedical Engineering and Center for Gene Regulation of Health and Disease (GRHD), Cleveland State University, Cleveland, Ohio 44115, United States

ABSTRACT: Glycan-binding molecules, such as lectins, are very important tools for characterizing, imaging, or targeting glycans and are often involved in either physiological or pathological processes. However, their availability is far less compared to the diversity of native glycans. Therefore, development of lectin mimetics with desired specificity and affinity is in high demand. Boronic acid reacts with 1,2- and 1,3-diols of saccharides in aqueous media through reversible boronate ester formation and are regarded as synthetic lectin mimetics. In this study, bovine serum albumin (BSA)−phenylboronic acid (PBA) conjugates were synthesized in a density-controlled manner by targeting both aspartic and glutamic acids to afford lectin mimetics with multivalent PBA, as multivalency is a key factor for glycan recognition in both specificity and affinity. The resultant BSA−PBA conjugates were characterized by sodium dodecyl sulfate polyacrylamide gel electrophoresis and matrix-assisted laser desorption/ionization time-of-flight mass spectrometry analysis. Their macrophage cell surface glycan-binding capacity was characterized by a competitive lectin-binding assay examined by flow cytometry, and 3-(4,5-di-methylthiazol-2-yl)-2,5-diphenyltetrazolium bromide assay showed biocompatibility. These novel lectin mimetics will find a broad range of applications as they can be wittingly modified, altering binding specificity and capacity.

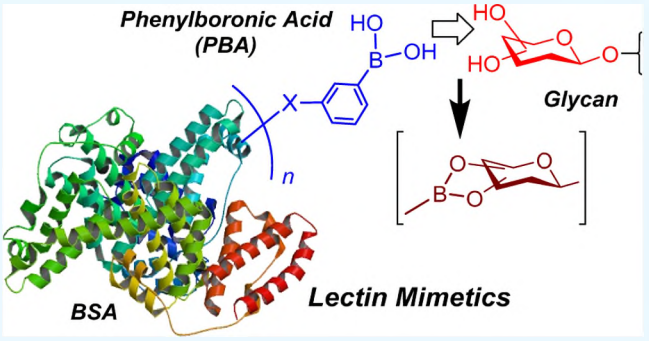

INTRODUCTION

Carbohydrate recognition is a crucial event in many biological processes.[1] For example, cell surface glycans, existing as glycoproteins, glycolipids, or proteoglycans, are involved in a variety of biological processes, including cellular adhesion, cell signaling, cell−cell communication, and immune response.[2−4] Cell surface glycans are highly associated with disease development, such as inflammation and cancer.[5,6] Over-expression of cell surface glycans is confirmed in cancer cells compared to healthy cells used as a control.[7] Therefore, sensitive profiling of cell surface glycans is highly demanded for basic glycomic advancement, clinical diagnostics, and therapeutic applications. In fact, the diversity and complexity of glycan structures, together with their crucial role in many physiological or pathological processes, require the development of new techniques for analysis. Lectins are carbohydrate-binding proteins having at least one noncatalytic domain that binds reversibly to a specific carbohydrate.[8] Due to their specificity, they have been employed to identify cell surface glycans and glycoconjugates. Fluorescently labeled lectins have been widely used as intracellular and extracellular labels for cellular glycan profiling.[9−11] Further, lectin arrays using lectins as probes are well established to determine specific glycan markers among different cell populations.[12] In addition, lectins are also used for cellular targeting, showing promise in biomedical applications, including targeting of apoptotic and autophagic pathways useful in anticancer therapies.[13] Although natural lectins are very important tools for glycoscience research and application, they also have major limitations, such as difficulty in production, instability toward rigorous use, high cost, and lack of availability.[14] Another limiting factor is low binding affinity and specificity leading to poor sensitivity for analytical assays because rarely is any glycan found at high abundance in a biological sample.[15] In an effort to mitigate these limitations, clustered or linked lectins have been explored because of the important role of multivalency in glycan−protein interactions.[16,17]

Boronic acids (BAs) react with 1,2- and 1,3-diols of saccharides in aqueous media through reversible boronate ester formation.[18−20] This interaction has been explored for potential applications in the analysis of glycans and glycoconjugates. So far, BA-containing ligands have been employed as artificial carbohydrate receptors,[21,22] membrane transport agents,[22] and cell surface carbohydrate recognition ligands.[23] It has been reported that phenylboronic acid (PBA) can selectively bind to the glycerol side chain of sialic acids (SAs) under physiological conditions, and the complex is stabilized through coordination of the amide NH or CO located at the C-5 position of SAs.[24] This anomalous binding profile of PBA strongly suggests an innovative molecular

Received: April 27, 2018
Accepted: July 5, 2018
Published: October 18, 2018

DOI: 10.1021/acsomega.8b00840
ACS Omega 2018, 3, 13467−13473

Scheme 1. Synthesis of BSA−PBA Conjugates

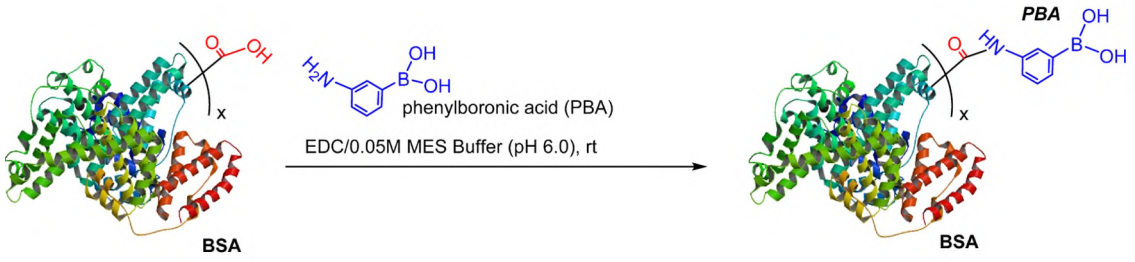

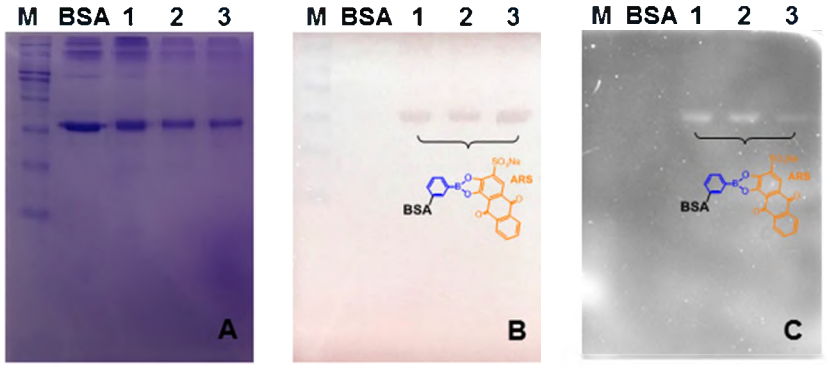

Figure 1. SDS-PAGE analysis of EDC coupling of BSA to 3-PBA. (A) All protein bands visualized by Coomassie blue staining. (B) BSA−PBA bands visualized by ARS staining. (C) Fluorescent images of conjugated BSA−PBA bands stained with ARS (M: protein molecular weight marker; BSA: bovine serum albumin; 1: BSA−PBA1; 2: BSA−PBA2; and 3: BSA−PBA3).

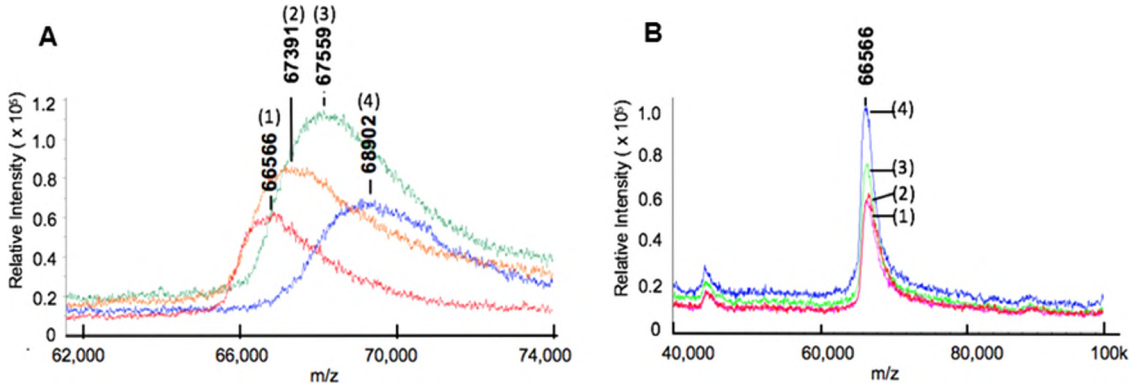

Figure 2. Characterization of BSA−PBA conjugates by MALDI-TOF MS. (A) MALDI-TOF MS-spectra of (1) BSA, (2) BSA−PBA1, (3) BSA−PBA2, and (4) BSA−PBA3 obtained by reacting BSA with PBA in different ratios in the presence of EDC; (B) MALDI-TOF MS spectra of (1) BSA and (2−4) BSA mixed with PBA in different ratios but without EDC.

targeting platform for selective recognition of cell surface SA residues of both glycoproteins and glycolipids. To further investigate the glycan-binding ability of multivalent lectin mimetics, we designed protein−PBA conjugates to elucidate cell surface SA capabilities and evaluate their application as synthetic lectin mimetics. Specifically, bovine serum albumin (BSA)−PBA conjugates were synthesized in a density-controlled manner by targeting both aspartic and glutamic acids to afford the lectin mimetics with multivalent PBA, as multivalence is a key factor for glycan−protein binding in both specificity and affinity. The resultant BSA−PBA conjugates were characterized by sodium dodecyl sulfate polyacrylamide gel electrophoresis (SDS-PAGE) and matrix-assisted laser desorption/ionization time-of-flight mass spectrometry (MALDI-TOF MS) analysis. Further, its cell surface glycan-binding capacity was confirmed by competitive lectin-binding assay examined by flow cytometry.

RESULTS AND DISCUSSION

Synthesis and Characterization of BSA−PBA Conjugates. Considering PBA's ability to reversibly bind 1,2- and 1,3-diols in aqueous media along with BSA's well-tolerated and widespread application, BSA−PBA conjugates were designed as lectin mimetics and were synthesized via *N*-(3-(dimethylamino)propyl)-*N*-ethylcarbodiimide hydrochloride (EDC) coupling. In this instance, amidation of carboxylic acids in BSA was followed by conjugation with 3-aminophenylboronic acid in the presence of EDC dissolved in 2-(*N*-morpholino)ethane sulfonic (MES) buffer (Scheme 1). The resultant BSA−PBA conjugates were purified on a Hi-Trap Sephadex G-25 column by using diH_2O as eluent. Different densities of BSA−PBA conjugates were synthesized by altering the ratio of PBA to BSA.

The resultant BSA−PBA conjugates were characterized by SDS-PAGE gel with Coomassie blue and Alizarin Red S (ARS)

DOI: 10.1021/acsomega.8b00840
ACS Omega 2018, 3, 13467−13473

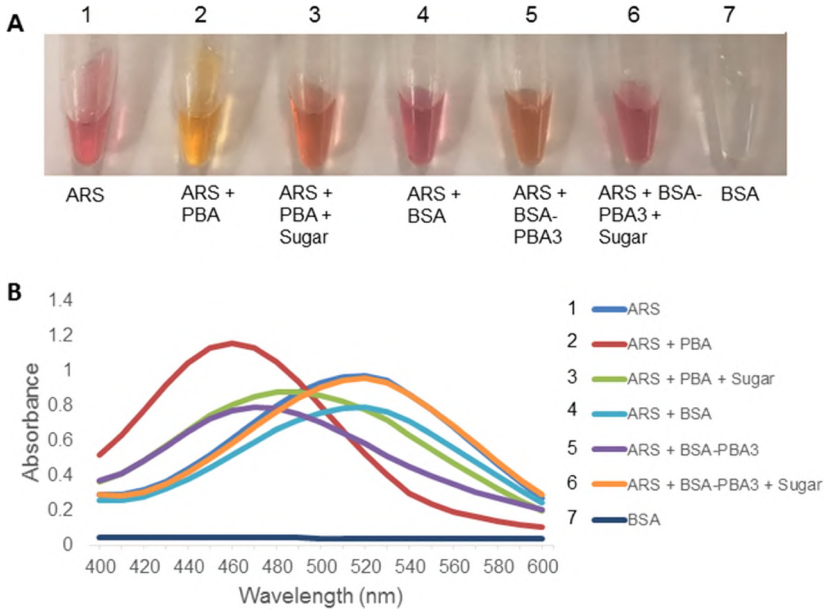

Figure 3. Alizarin Red S (ARS) displacement assay in PBS (pH 7.4). (A) ARS solutions after incubation with PBA or BSA−PBA conjugates and then fructose: (1) ARS, (2) ARS mixed with free PBA, (3) ARS mixed with free PBA, then with fructose, (4) ARS mixed with free BSA, (5) ARS mixed with BSA−PBA, (6) ARS mixed with BSA, then with fructose, (7) BSA. (B) UV spectra of ARS solutions after incubation with PBA or BSA−PBA conjugates then fructose: (1) ARS, (2) ARS mixed with free PBA, (3) ARS mixed with free PBA, then with fructose, (4) ARS mixed with free BSA, (5) ARS mixed with BSA−PBA, (6) ARS mixed with BSA−PBA, then with fructose, (7) BSA.

staining assay. First, BSA−PBA conjugates were characterized by SDS-PAGE, where they showed an increase in molecular weight (Figure 1A). ARS binds to PBA in a 1:1 ratio, and a dramatic change in color and UV−vis and fluorescent absorption spectra can be monitored. Therefore, the BSA−PBA conjugates characterized on SDS-PAGE were stained with ARS. As shown in Figure 1B, clear yellowish spots of all three BSA−PBA conjugates were observed, but not for unmodified BSA. In the same respect, fluorescent signals were obtained for all three BSA−PBA conjugates, but not for the BSA on the gel under fluorescence scanner (Figure 1C). These data confirmed that the BSA−PBA conjugates were successfully synthesized.

Next, MALDI-TOF MS was used to characterize the BSA−PBA conjugates using a sinapic acid matrix with a Bruker Autoflex III mass spectrometer. The mass spectrum acquired for unmodified BSA showed the typical profile of a nonglycosylated, nonfunctionalized protein. The molecular ion peak was broadly dispersed over 66 430 Da due to an isotopic effect relative to the size of the protein (Figure 2A). The m/z ratio increases and peak position shifts to the right as BSA functionalized with PBA and the amount of shift is directly correlated to the amount of PBA conjugated to BSA (Figure 2A(2,3,4)). As a result, three BSA−PBA conjugates were obtained with the PBA/BSA ratio increase in the reactions, affording BSA−PBA1 determined to have 5 PBA functionalities, BSA−PBA2 to have 10 PBA, and BSA−PBA3 to have 15 PBA functionalities. The MALDI-TOF MS spectra of BSA (1) and BSA mixed with PBA in different ratios but without EDC (Figure 2B(2−4)) showed no molecular weight change, indicating no PBA conjugation occurred. These data further confirmed that the BSA−PBA conjugates were successfully synthesized.

Carbohydrate-Binding Capacity of BSA−PBA Conjugates. The carbohydrate-binding capacity of BSA−PBA conjugates was examined by ARS displacement assay, which has been used extensively to quantify boronic acid and carbohydrate-binding capabilities.[25−27] Briefly, ARS shows a color change from red to yellow when bound to BSA−PBA and shifts the UV absorption wavelength from 520 to 460 nm in phosphate-buffered saline (PBS, pH 7.4). When adding a (0.1 M) fructose, the fructose−boronic acid complex forms, releasing ARS with the color changing from yellow back to red and the wavelength shifting back to 520 nm (Figure 3B).

Silica beads have been widely used as small, rigid particles for high-performance affinity chromatography and are capable of withstanding high flow rates and/or pressures. Recently, surface-functionalized silica beads have received widespread attention for affinity chromatography applications.[28,29] In the present study, BSA−PBA conjugates were immobilized onto maleimide-functionalized silica beads, and their respective carbohydrate-binding affinity and specificity were investigated. First, BSA−PBA was dissolved in 0.1 mM PBS (pH 7.4). This BSA−PBA solution was added to commercially available maleimide-functionalized silica beads (Sigma) and the thiol−maleimide coupling reaction was allowed at room temperature for 4 h. Then, the unreacted BSA−PBA was removed by washing the silica beads with 0.1 mM PBS (pH 7.4) three times to afford BSA−PBA-functionalized silica beads (SB−BSA−PBA). Then, the resultant SB−BSA−PBA was characterized by ARS binding assays compared to BSA-modified silica beads and untreated maleimide-functionalized silica beads as well. As a result, SB−BSA−PBA incubated with ARS solution showed strong ARS binding compared to unmodified silica beads and BSA-modified silica beads incubated with the same ARS solution.

Next, the SB−BSA−PBA was used to evaluate the carbohydrate-binding affinity and specificity by ARS displacement assay. First, SB−BSA−PBA (15 mg) was incubated with ARS (0.1 μM) in PBS (pH 7.4) at room temperature for 30 min. After centrifugation, the supernatant containing unreacted ARS was removed by a pipette and the silica beads were washed three times with PBS (pH 7.4). Among the BSA−PBA

DOI: 10.1021/acsomega.8b00840
ACS Omega 2018, 3, 13467−13473

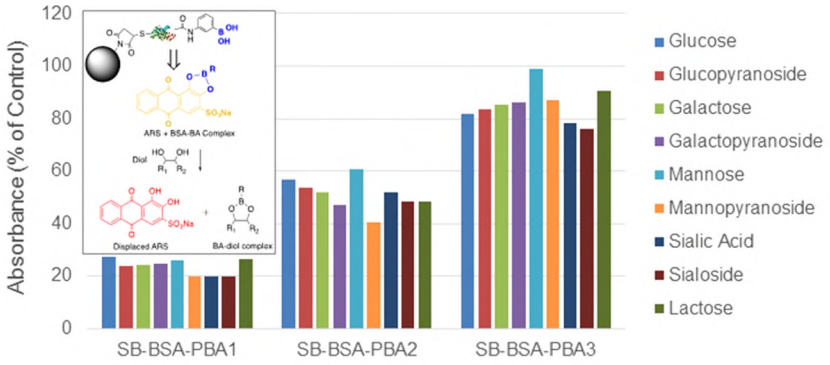

Figure 4. Carbohydrate-binding capacity of BSA−PBA measured by ARS replacement assay immobilized on silica gel beads. BSA−PBA conjugates were immobilized onto maleimide-functionalized silica gel, incubated with ARS, followed by washing and incubation with monosaccharides and their *O*-methyl glycoside. Absorbance at 520 nm was recorded for the free ARS replaced by sugars from the beads (sialic acid: Neu5Ac, sialoside: 2-α-*O*-Methyl glycoside of Neu5Ac).

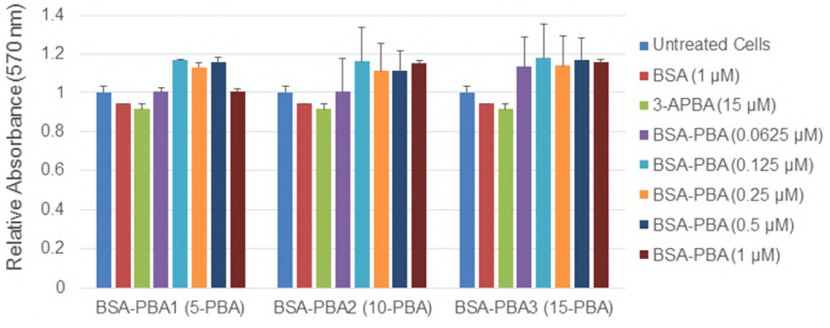

Figure 5. MTT assay. Raw 264.7 cells were incubated with BSA, PBA, and BSA−PBA conjugates for 24 h at 37 °C. The error bars represent one standard deviation of the averaged cell percent viability (n = 3).

conjugates used, the BSA−PBA3-modified silica beads displayed the highest binding of ARS, as it has higher density of PBA compared to BSA−PBA1 and BSA−PBA2 (Figure 4). The BSA-modified silica beads and silica gel beads alone showed no ARS released and were subtracted as controls during the experiment. To support this evidence, ARS displacement by the introduction of a high concentration (0.1 M) of saccharides was investigated. This method has been used in the past to determine multiple facets of PBA binding to include saccharide kinetics, affinity, and specificity.[30] The ARS-bound SB−BSA−PBA was incubated with free monosaccharides solution (0.1 M) in PBS (pH 7.4) at room temperature for 30 min to displace the bound ARS from the SB−BSA−PBA. In addition, their *O*-methyl glycosides of all sugars were investigated, and *O*-methyl glycosides mimic the native form of sugars in glycan chains linked via *O*-glycosylation. The displaced ARS was subjected to UV−vis spectroscopy, and the corresponding absorbance data were in direct correlation with the amount of ARS released from the SB−BSA−PBA, which is the indicator of the binding affinity and specificity of BSA−PBA conjugates to free monosaccharides and their *O*-methyl glycosides. As a result, BSA−PBA3 conjugates with the highest density of PBA showed the highest binding capacity for both free monosaccharides and their *O*-methyl glycosides compared to BSA−PBA1- and BSA−PBA2-modified silica beads (Figure 4). However, there was no significant difference observed regarding specificity for both monosaccharides and their *O*-methyl glycosides. This result indicates that the SB−BSA−PBA binding is dependent on the number of PBAs on BSA, but it is unknown based on this assay if the saccharide truly makes a difference.

Evaluation of Biocompatibility of BSA−PBA Conjugates. The relative cytotoxicity of BSA−PBA conjugates toward Raw 264.7 cells was estimated by an 3-(4,5-dimethylthiazol-2-yl)-2,5-diphenyltetrazolium bromide (MTT) viability assay. Briefly, Raw 264.7 cells were seeded into 96-well plates at a density of 1×10^4 per well in 200 μL of medium. After 24 h of incubation, the culture medium was removed and replaced with 200 μL of media containing serial dilutions of BSA−PBA conjugates. The cells were grown for another 24 h. Then, 200 μL of 0.5 mg/mL MTT assay stock solution, in phenol red free medium, was added to each well. After incubating the cells for 4 h, the medium having unreacted dye was removed carefully. The obtained purple formazan crystals were dissolved in 100 μL SDS-HCl per well, and the absorbance was measured at 570 nm. As a result, no apparent cytotoxicity to Raw 264.7 cells was observed up to a high concentration of 1 μM for all three BSA−PBA conjugates. Instead, certain level of cell proliferation was observed for higher concentration of the three BSA−PBA conjugates (Figure 5).

Evaluation of Cell Surface Glycan-Binding Capability of BSA−PBA Conjugates. SAs are found linked to galactose residues by either α-2,3 or α-2,6 linkage on the cell surface.[31] In this study, the binding capacity of BSA−PBA conjugates to cell surface SA was determined via competitive inhibition of the binding of lectins that specifically recognize SA by flow cytometry analysis. First, Raw 264.7 cells were incubated with BSA−PBA conjugates for 90 min, followed by incubation with MAA-FITC and SNA-FITC, which specifically bind to α-2,3 and α-2,6-linked SAs, respectively.[32] From the flow cytometry study (Figure 6), MAA-FITC showed very strong binding

DOI: 10.1021/acsomega.8b00840
ACS Omega 2018, 3, 13467−13473

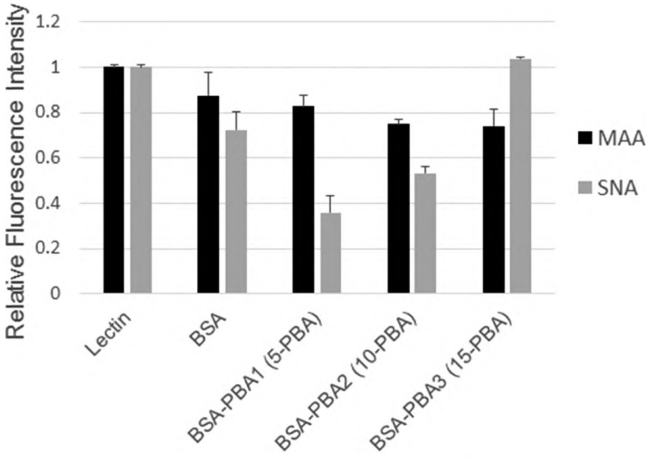

Figure 6. Cell surface SA binding capacity of BSA–PBA lectin mimetics. Raw 264.7 cells were incubated with BSA, BSA–PBA conjugate (5 μg/mL), followed by MAA and SNA lectin (10 μg/mL). The error bars indicate one standard deviation of the averaged fluorescence intensity (n = 3).

compared to SNA-FITC on the cell surface of Raw 264.7 cells, cultured under the normal condition. And it was apparent that BSA–PBA could inhibit binding of MAA-FITC by blocking available binding sites with respect to the number of PBA residues available from BSA–PBA for interaction. SNA-FITC, on the other hand, showed a drastic decrease in binding when incubated with BSA–PBA1 cells, followed by an increase in fluorescence intensities with BSA–PBA2 and BSA–PBA3, which have high PBA content. This inverse relationship may be due to PBA location or geometry is different in these three BSA–PBA conjugates and their ability to bind cell surface SAs may be different, thereby having different inhibition capacities for SNA binding. It is known that MAA and SNA specifically bind to α-2,3- and α-2,6-linked SAs as they have different binding sites and different SA geometry preferences.[32] It may also be possible that BSA–PBA2 and BSA–PBA3 may induce more expression of α-2,6-linked SAs, resulting in an increase in the fluorescence intensity of the SNA-FITC. This phenomenon is correlated to the MTT assay data (Figure 5), in which BSA–PBA2 and BSA–PBA3 conjugates were able to proliferate the concentration of cells. To confirm all of these speculations, we plan to design more BSA–PBA conjugates and characterize their PBA conjugation location and quantify cell surface SA expression of macrophage upon incubation with these lectin mimetics in detail in our future study. To explain the reduction in fluorescence intensity caused by the BSA control, it is possible that the BSA may limit this effect, showing true 100% lectin binding.

CONCLUSIONS

BSA–PBA conjugates were successfully synthesized, and their glycan recognition has been demonstrated as lectin mimetics. The conjugates were synthesized in a density-controlled manner using traditional EDC coupling, affording amide derivatives from carboxylic acid residues within the BSA. The BSA–PBA conjugates were characterized by SDS-PAGE and MALDI-TOF MS. The BSA–PBA conjugates were immobilized onto maleimide-functionalized silica gel via thiol–maleimide interactions and used to study the sugar-binding capacity by ARS displacement assay. Evaluation of biocompatibility using an MTT assay showed no effect on cell viability after 24 h. Finally, cellular studies confirmed the binding of BSA–PBA conjugates to the cell surface SA of Raw 264.7 cells based on the inhibition of lectin–FITC binding. These lectin mimetics have more favorable properties compared to natural lectin in terms of toxicity and inherent immunogenicity and will provide a valuable tool for future glycomics, biosensor, and immunomodulation research and applications.

EXPERIMENTAL SECTION

Materials and Instruments. All solvents and reagents were purchased from commercial sources and were used as received, unless otherwise noted. Deionized water was used as a solvent in all procedures. 3-Aminophenylboronic acid, Alizarin Red S (ARS), BSA, *N*-(3-(dimethylamino)propyl)-*N*-ethylcarbodiimide, 3-(4,5-di-methylthiazol-2-yl)-2,5-diphenyltetrazolium bromide (MTT), and maleimide-functionalized silica beads and Sephadex G-25 were purchased from Sigma-Aldrich (St. Louis, MO). Glucose, methyl β-*O*-glucopyranoside, galactose, methyl β-*O*-galactopyranoside, mannose, methyl α-*O*-mannopyranoside, sialic acid, and lactose were purchased from Sigma-Aldrich (St. Louis, MO). MAA-FITC and SNA-FITC were purchased from Bio-World (Dublin, OH). 2-α-*O*-Methyl glycoside of Neu5Ac was synthesized by a literature method.[33]

Synthesis of BSA–PBA Conjugates. BSA (100 mg, 30 μM) and 3-aminophenylboronic acid (30 mg, 400 mM) were dissolved in 5 mL of 0.05 M 2-(*N*-morpholino)ethane sulfonic acid buffer (MES; pH 6.0). To this mixture, *N*-(3-(dimethylamino)propyl)-*N*-ethylcarbodiimide hydrochloride (EDC; 15 mg, 80 μM) was added under constant stirring and allowed to react overnight at room temperature. Then, the reaction mixture was subjected to a Sephadex G-25 column with diH_2O as eluent for purification and lyophilized. BSA–PBAs of different densities were prepared using the same procedure as above by changing the ratios of BSA to PBA. Characterization was carried out by SDS-PAGE using both Coomassie blue and ARS as stains and imaged on a Typhoon 9410 Variable Mode Imager.

Matrix-Assisted Laser Desorption Ionization/Time-of-Flight Mass Spectrometry (MALDI-TOF MS). The high purities and expected structures of the conjugated BSA–PBA derivatives were verified by MALDI-TOF MS using a Bruker Autoflex III MALDI-TOF mass spectrometer. The sample was applied onto the target plate using the dry droplet technique, in which 1 μL of sample containing 1 μg of total protein in 0.1% trifluoroacetic acid (TFA) was mixed with 1 μL of matrix (20 mg/mL sinappic acid in 0.1% TFA, 40% acetonitrile). The spots were dried at room temperature to allow sample crystallization prior to insertion into the instrument, and the spectrum was obtained in linear mode.

Immobilization of BSA–PBA onto Silica Beads. BSA–PBA (45 mg, 2 mM) and maleimide-functionalized silica beads (250 mg) were incubated in PBS (3 mL, 0.1 M, pH 7.4) for 4 h at room temperature. The reaction mixture was then centrifuged and washed with 0.1 M PBS (pH 7.4) three times to remove unreacted BSA–PBA. The same procedure was used for immobilization of all BSA–PBA conjugates as well as unmodified BSA.

Alizarin Red S Binding and Displacement Assay of BSA–PBA on Silica Beads. BSA–PBA-modified silica beads (15 mg) were incubated with ARS (400 μM) in PBS (1 mL, 0.1 M, pH 7.4) for 30 min at room temperature and

DOI: 10.1021/acsomega.8b00840
ACS Omega 2018, 3, 13467–13473

centrifuged to remove unreacted ARS. The beads were then centrifuged and washed with 0.1 M PBS (pH 7.4) three times to remove unreacted or loosely bound ARS, followed by incubation of these silica beads with 100 mM sugar solutions (glucose, methyl β-*O*-glucopyranoside, galactose, methyl β-*O*-galactopyranoside, mannose, methyl α-*O*-mannopyranoside, Neu5Ac, 2-α-*O*-methyl glycoside of Neu5Ac, and lactose) in 0.1 M PBS (1 mL, pH 7.4) for 30 min at room temperature. Supernatant containing displaced ARS was removed after centrifugation and subjected to UV−vis spectroscopy. The absorbance of each well was measured on a microplate reader (Molecular Devices Spectrometer Plus 384) at 520 nm.

Cell Culture Methods. Raw 264.7 cells (ATCC) were cultured using Dulbecco's modified Eagle's medium supplemented with 10% fetal bovine serum and 1% penicillin/streptavidin at 37 °C in a humidified 5% CO_2 atmosphere. Subculture was performed when the cells had 80−90% confluence using trypsin−ethylenediaminetetraacetic acid.

MTT Assay. The biocompatibility of the BSA−PBA conjugates was measured by 3-(4, 5-di-methylthiazol-2-yl)-2, 5-diphenyltetrazolium bromide (MTT) assay. Raw 264.7 cells (ATCC) were seeded in 96-well plates at a density of 1×10^4 cells/well in medium and incubated for 24 h at 37 °C (5% CO_2). After 24 h, the medium was replaced with a new medium, supplemented with BSA−PBA conjugates, at varying concentrations (0.062, 0.125, 0.25, 0.5, and 1 μM). After an additional 24 h, the cell medium was again removed and 100 μL of 5 mg/mL MTT solution was added to each well, and the plates were incubated for 4 h. The MTT solution was removed and 100 μL of 1SDS-HCl per well was added to solubilize the precipitate, and the plates were shaken for 10 min. The absorbance of each well was measured on a microplate reader at 520 nm.

Competitive Inhibition of Lectin Binding to Macrophage Cell Surface SA by Flow Cytometry Analysis. Raw 264.7 cells were seeded at 4×10^5 cells/well (5 mL tubes) and treated with BSA−PBA conjugates for 90 min. The cells were then washed three times with cold phosphate-buffered saline (PBS; 0.2 mL, pH 7.4) and suspended in 50 μL of PBS (pH 7.4) containing MAA-FITC (10 μg/mL) or SNA-FITC (10 μg/mL). After incubation for 30 min at room temperature, the cells were washed with cold PBS (pH 7.4) three times and resuspended in 500 μL of the same buffer for flow analysis. A minimum of 10 000 cells were measured each time. The fluorescence intensity of fluorescein-labeled lectins was subtracted from the intensity of the cell−lectin complex. All experiments were carried out in triplicate and spectra were obtained on a BD FACSCanto II Flow Cytometer.

AUTHOR INFORMATION

Corresponding Author

*E-mail: x.sun55@csuohio.edu.

ORCID

Xue-Long Sun: 0000-0001-6483-1709

Notes

The authors declare no competing financial interest.

ACKNOWLEDGMENTS

This study was partially supported by Faculty Research Fund from the Center for Gene Regulation in Health and Disease (GRHD) (X.-L.S.) at Cleveland State University supported by Ohio Department of Development (ODOD) as well as Dissertation Research Award (DRA, J.W.) at Cleveland State University.

REFERENCES

(1) Jin, S.; Cheng, Y.; Reid, S.; Li, M.; Wang, B. Carbohydrate recognition by boronolectins, small molecules, and lectins. *Med. Res. Rev.* **2010**, *30*, 171−257.

(2) Marth, J. D.; Grewal, P. K. Mammalian glycosylation in immunity. *Nat. Rev. Immunol.* **2008**, *8*, 874.

(3) Gu, J.; Isaji, T.; Xu, Q.; Kariya, Y.; Gu, W.; Fukuda, T.; Du, Y. Potential roles of N-glycosylation in cell adhesion. *Glycoconjugate J.* **2012**, *29*, 599−607.

(4) Varki, A. Biological roles of oligosaccharides: all of the theories are correct. *Glycobiology* **1993**, *3*, 97−130.

(5) Pomin, V. H. Sulfated glycans in inflammation. *Eur. J. Med. Chem.* **2015**, *92*, 353−369.

(6) Christiansen, M. N.; Chik, J.; Lee, L.; Anugraham, M.; Abrahams, J. L.; Packer, N. H. Cell surface protein glycosylation in cancer. *Proteomics* **2014**, *14*, 525−46.

(7) Han, E.; Ding, L.; Ju, H. Highly sensitive fluorescent analysis of dynamic glycan expression on living cells using glyconanoparticles and functionalized quantum dots. *Anal. Chem.* **2011**, *83*, 7006−7012.

(8) Peumans, W. J.; Van Damme, E. J. Lectins as plant defense proteins. *Plant Physiol.* **1995**, *109*, 347−352.

(9) Sommer, U.; Rehn, B.; Kressin, M. Light and electron microscopic investigation of the lectin-binding pattern in the oxyntic gland region of bovine abomasum. *Ann. Anat.* **2001**, *183*, 135−143.

(10) Laurila, P.; Virtanen, I.; Wartiovaara, J.; Stenman, S. Fluorescent antibodies and lectins stain intracellular structures in fixed cells treted with nonionic detergent. *J. Histochem. Cytochem.* **1978**, *26*, 251−257.

(11) Shimizu, T.; Nettesheim, P.; Mahler, J. F.; Randell, S. H. Cell type-specific lectin staining of the tracheobronchial epithelium of the rat: quantitative studies with Griffonia simplicifolia I isolectin B4. *J. Histochem. Cytochem.* **1991**, *39*, 7−14.

(12) Nand, A.; Singh, V.; Wang, P.; Na, J.; Zhu, J. Glycoprotein profiling of stem cells using lectin microarray based on surface plasmon resonance imaging. *Anal. Biochem.* **2014**, *465*, 114−120.

(13) Fu, L. L.; Zhou, C. C.; Yao, S.; Yu, J. Y.; Liu, B.; Bao, J. K. Plant lectins: targeting programmed cell death pathways as antitumor agents. *Int. J. Biochem. Cell Biol.* **2011**, *43*, 1442−1449.

(14) Bicker, K. L.; Sun, J.; Lavigne, J. J.; Thompson, P. R. Boronic acid functionalized peptidyl synthetic lectins: Combinatorial library design, peptide sequencing, and selective glycoprotein recognition. *ACS Comb. Sci.* **2011**, *13*, 232−243.

(15) Haab, B. B. Using lectins in biomarker research: Addressing the limitations of sensitivity and availability. *Proteomics: Clin. Appl.* **2012**, *6*, 346−350.

(16) Lee, Y. C.; Lee, R. T. Carbohydrate-Protein Interactions: Basis of Glycobiology. *Acc. Chem. Res.* **1995**, *28*, 321−327.

(17) Lee, R. T.; Lee, Y. C. Affinity enhancement by multivalent lectin−carbohydrate interaction. *Glycoconjugate J.* **2000**, *17*, 543−551.

(18) Li, J.; Wang, Z.; Li, P.; Zong, N.; Li, F. A sensitive non-enzyme sensing platform for glucose based on boronic acid−diol binding. *Sens. Actuators, B* **2012**, *161*, 832−837.

(19) Okamoto, T.; Tanaka, A.; Watanabe, E.; Miyazaki, T.; Sugaya, T.; Iwatsuki, S.; Inamo, M.; Takagi, H. D.; Odani, A.; Ishihara, K. Relative kinetic reactivities of boronic acids and boronate ions toward 1,2-diols. *Eur. J. Inorg. Chem.* **2014**, *2014*, 2389−2395.

(20) Craig, S. Synthesis and evaluation of aryl boronic acids as fluorescent artificial receptors for biological carbohydrates. *Bioorg. Chem.* **2012**, *40*, 137−142.

(21) Heinrichs, G.; Schellenträger, M.; Kubik, S. An enantioselective fluorescence sensor for glucose based on a cyclic tetrapeptide containing two boronic acid binding sites. *Eur. J. Org. Chem.* **2006**, *2006*, 4177−4186.

(22) Westmark, P. R.; Smith, B. D. Boronic acids selectively facilitate glucose transport through a lipid bilayer. *J. Am. Chem. Soc.* **1994**, *116*, 9343−9344.

DOI: 10.1021/acsomega.8b00840
ACS Omega 2018, 3, 13467−13473

(23) Yan, J.; Fang, H.; Wang, B. Boronolectins and fluorescent boronolectins: an examination of the detailed chemistry issues important for the design. *Med. Res. Rev.* **2005**, *25*, 490−520.
(24) Regueiro-Figueroa, M.; Djanashvili, K.; Esteban-Gómez, D.; Chauvin, T.; Tóth, É; de Blas, A.; Rodríguez-Blas, T.; Platas-Iglesias, C. Molecular Recognition of Sialic Acid by Lanthanide(III) Complexes through Cooperative Two-Site Binding. *Inorg. Chem.* **2010**, *49*, 4212−4223.
(25) Springsteen, G.; Wang, B. Alizarin Red S. as a general optical reporter for studying the binding of boronic acids with carbohydrates. *Chem. Commun.* **2001**, 1608−1609.
(26) Kubo, Y.; Ishida, T.; Kobayashi, A.; James, T. D. Fluorescent alizarin-phenylboronic acid ensembles: design of self-organized molecular sensors for metal ions and anions. *J. Mater. Chem.* **2005**, *15*, 2889−2895.
(27) Maue, M.; Schrader, T. A Color Sensor for Catecholamines. *Angew. Chem., Int. Ed.* **2005**, *44*, 2265−2270.
(28) Ivanov, A. E.; Panahi, H. A.; Kuzimenkova, M. V.; Nilsson, L.; Bergenstahl, B.; Waqif, H. S.; Jahanshahi, M.; Galaev, I. Y.; Mattiasson, B. Affinity adhesion of carbohydrate particles and yeast cells to boronate-containing polymer brushes grafted onto siliceous supports. *Chem. - Eur. J.* **2006**, *12*, 7204−7214.
(29) Liu, L.; Zhang, Y.; Zhang, L.; Yan, G.; Yao, J.; Yang, P.; Lu, H. Highly specific revelation of rat serum glycopeptidome by boronic acid-functionalized mesoporous silica. *Anal. Chim. Acta* **2012**, *753*, 64−72.
(30) Narla, S. N.; Pinnamaneni, P.; Nie, H.; Li, Y.; Sun, X. L. BSA-boronic acid conjugate as lectin mimetics. *Biochem. Biophys. Res. Commun.* **2014**, *443*, 562−7.
(31) Varki, A. Loss of N-glycolylneuraminic acid in humans: Mechanisms, consequences, and implications for hominid evolution. *Am. J. Phys. Anthropol.* **2001**, *116*, 54−69.
(32) Sharon, N.; Lis, H. History of lectins: from hemagglutinins to biological recognition molecules. *Glycobiology* **2004**, *14*, 53R−62R.
(33) Kononov, L.; Chinarev, A.; Zinin, A. I.; Gobble, C. *Carbohydrate Chemistry: Proven Synthetic Methods. Synthesis of α-N-Acetylneuraminic Acid Methyl Glycoside*; Marel, G., Codee, J., Eds.; CRC Press: Florida, 2014; pp 197−206.

DOI: 10.1021/acsomega.8b00840
ACS Omega 2018, 3, 13467−13473